NeuroImage 264 (2022) 119707

Contents lists available at ScienceDirect

NeuroImage

journal homepage: www.elsevier.com/locate/neuroimage

Subjective time is predicted by local and early visual processing

Yelena Tonoyan*, Michele Fornaciai*, Brent Parsons, Domenica Bueti

International School for Advanced Studies (SISSA), Via Bonomea 265, Trieste, TS 34136, Italy

ARTICLE INFO

Keywords:
Time perception
Motion adaptation
Duration compression
EEG
Neural decoding

ABSTRACT

Time is as pervasive as it is elusive to study, and how the brain keeps track of millisecond time is still unclear. Here we addressed the mechanisms underlying duration perception by looking for a neural signature of subjective time distortion induced by motion adaptation. We recorded electroencephalographic signals in human participants while they were asked to discriminate the duration of visual stimuli after different types of translational motion adaptation. Our results show that perceived duration can be predicted by the amplitude of the N200 event-related potential evoked by the adapted stimulus. Moreover, we show that the distortion of subjective time can be predicted by the activity in the Beta band frequency spectrum, at the offset of the adaptor and during the presentation of the subsequent adapted stimulus. Both effects were observed from posterior electrodes contralateral to the adapted stimulus. Overall, our findings suggest that local and low-level perceptual processes are involved in generating a subjective sense of time.

1. Introduction

Time is pervasive in all human activities, and our sense of time is foundational to our very existence. For instance, knowing the precise time at which to reach out and grasp a prey or to cross a busy street requires an accurate estimate of the passage of time. Despite such foundational importance, and the growing number of studies on this topic, how the brain processes and represents time is still unclear. Several accounts of time perception have been proposed in the past decades, involving brain mechanisms like a centralized pacemaker-accumulator (Treisman et al., 1990), detectors of oscillatory activity in the striatum (Meck and Benson, 2002), or the intrinsic dynamic of sensory neurons (Buonomano and Maass, 2009). Although the pacemaker-accumulator remains the most popular model – as it can account for many properties of time perception – none of these frameworks has yet reached general consensus. Conversely, evidence showing different properties of time perception at different time scales suggests the existence of multiple time-keeping mechanisms (Fornaciai et al., 2018; Karmarkar and Buonomano, 2007; Spencer et al., 2009; Wiener et al., 2011; see also Merchant and de Lafuente 2014).

Crucial to understand the mechanisms of time perception is to assess how physical temporal information is translated into a *subjective* sense of time. Indeed, perceived time often deviates from physical time, showing that temporal processing is malleable and prone to distortions. For instance, the perceived duration of a stimulus is strongly modulated by its physical properties, like motion (Brown, 1995; Kanai et al., 2006), size (Xuan et al., 2007), numerosity (Javadi and Aichelburg, 2012; Togoli et al., 2021, 2022), the context in which the stimulus is presented (Fornaciai et al., 2018; Karmarkar and Buonomano, 2007; Kristjánsson et al., 2007; Spencer et al., 2009), and also by motor actions (e.g., Merchant and Yarrow, 2016). Understanding the neural pathway leading to a subjective sense of time and the mechanisms responsible for temporal distortions is thus essential to reach a deeper understanding of time perception.

Here, we leverage the temporal distortions induced by motion adaptation to assess the brain processes linked to the perception of time. Indeed, it has been shown that adaptation to fast motion strongly reduces the apparent duration of a subsequent stimulus (Ayhan et al., 2009; Bruno et al., 2010; Burr et al., 2007; Fornaciai et al., 2016; Johnston et al., 2006a; Latimer et al., 2014) – an effect named "duration compression." While the properties of this adaptation effect are debated – especially concerning whether it occurs in a retinotopic (Bruno et al., 2010; Latimer et al., 2014) or spatiotopic (Burr et al., 2007; Burr et al., 2011) reference frame – it nevertheless offers a powerful tool to understand the brain mechanisms underlying our subjective sense of time. Indeed, motion adaptation represents the ideal technique in this context, for three main reasons. First, it typically yields strong distortions in perceived duration, with a compression of up to 20–30% in previous studies (e.g., Fornaciai et al., 2016), which is a necessary condition to be able to achieve robust and systematic behavioural effects and to relate them to changes measured at the neural level. Second, motion adaptation can be delivered in different forms, which are more or less effective depending for instance on the speed of the motion adaptor (e.g., Johston et al., 2006) and the relative direction of adaptor and adapted stimuli (Bruno et al., 2013). All these features thus give us the opportunity to potentially measure a parametric modulation of perceived du-

* Corresponding authors.
E-mail addresses: ytonoyan@sissa.it (Y. Tonoyan), mfornaci@sissa.it (M. Fornaciai).

https://doi.org/10.1016/j.neuroimage.2022.119707.
Received 18 April 2022; Received in revised form 14 October 2022; Accepted 20 October 2022
Available online 27 October 2022.

ration and its neural signature according to the effectiveness of adaptation. Third, the effect has been shown to be spatially localised to the position of the adaptor stimulus, which, in this context, is essential to have proper control conditions for potential spurious effects on brain activity. Namely, the spatial selectivity of the effect allows us to make sure that what we are measuring is a specific effect of adaptation on the processing of the adapted stimulus, and not, for instance, a general lingering trace of the adaptor stimulus processing or even a mnemonic representation of the adaptor stimulus itself.

To assess the neural signature of subjective time, we asked participants to perform a duration discrimination task (i.e., comparing the duration of a constant reference stimulus and a variable test duration) during electroencephalographic (EEG) recording. Crucially, in different conditions, participants were adapted to a fast (20 deg/s) or a slow (5 deg/s) moving stimulus, delivered to the same retinotopic or spatiotopic (i.e., screen) coordinates of the reference stimulus, or in a neutral location.

Our central goal is to assess how these different adaptation conditions affect the perceived duration of a physically identical stimulus (i.e., the reference stimulus), and to identify a neural signature of these perceptual distortions. Concerning the neural signature of subjective time, we had two main hypotheses. First, as we employed motion adaptation to bias perceived duration, we posited that the neural responses to motion adaptation might also be involved in duration distortion. In terms of event-related potentials (ERPs), previous studies show that the N200 component recorded at posterior EEG channels reflects motion processing and the effect of motion adaptation (Hoffmann et al., 1999; Hoffmann et al., 2001). The N200 thus represents our main target ERP component. Second, in line with previous results showing the involvement of the Beta frequency band in time perception (e.g., Kononowicz and Van Rijn, 2015; Kulashekhar et al., 2016), we posited that adaptation might distort perceived duration by modulating brain activity in the Beta band. To address this hypothesis, we thus assessed the power of Beta band activity during the adapted stimulus (i.e., the fixed duration reference stimulus) to see if and how Beta band activity was affected by adaptation and whether it could predict changes in perceived duration. Moreover, to explore potential links between Beta band frequency changes occurring during the reference stimulus and well before its presentation, during the adaptation phase itself, we also checked for changes in spectral power during the presentation of the adaptor stimulus (from its onset to offset).

To preview, the ERP analysis first shows that the amplitude of the N200 component recorded from posterior electrodes during the adapted stimulus is affected by motion adaptation, and can predict the perceived time distortion induced by adaptation. On the other hand, another component potentially associated with time perception, the contingent negative variation (CNV), does not show such a relationship. Moreover, our results show that motion adaptation affects the power of brain activity in the Beta band recorded at posterior electrodes, and that such changes in power at the adaptation offset and early during the reference stimulus presentation (adapted stimulus) successfully predict perceptual distortions. Importantly, these effects are localised to EEG channels contralateral to the stimuli. These results suggest that the emergence of subjective time is linked to processes starting locally and relatively early in the visual processing stream.

2. Materials and methods

2.1. Subjects

The experiment was conducted on 32 healthy subjects (18 females; mean age (± SD) = 25 ± 0.37; 30 out 32 right-handed participants), naïve to the purpose of the experiment, none of them reporting any neurological disease. Participants gave their written informed consent before taking part in the study, and were compensated for their participation with 12 Euro/hour. The study was carried out in accordance with the Declaration of Helsinki, and was approved by the local ethics committee of the Scuola Internazionale Superiore di Studi Avanzati (SISSA). Note that the sample size of the present study was chosen to be equal to the sample included in a previous study by Kononowicz and Van Rijn (2015), which shares a similar goal with the present study: addressing the involvement of Beta-band activity in time perception. Concerning the behavioural effect of adaptation, previous psychophysical studies typically tested relatively small samples of subjects (i.e., 11 in Burr et al., 2007, and 6 in Ayhan et al., 2009, for example). We thus opted for a sample size that was appropriate for an EEG experiment and was also large enough to reliably assess the behavioural effect of adaptation.

2.2. Apparatus and stimuli

The participants performed the experiment sitting in front of an LCD monitor (60 × 34 cm; 100 Hz refresh rate, resolution = 1920 × 1080 pixels; distance from the screen = 80 cm) where the stimuli were displayed. The stimuli used (i.e., adaptor, reference, and test) were arrays of black and white moving dots (number of dots = 50; 50%/50% of black and white dots; 100% contrast; dot radius = 5 pixels) presented in a circular area with a radius of 3.25 deg, with their initial position determined randomly. Each dot had a limited lifetime, and was replaced by another, randomly positioned dot after moving for 5 frames (50 ms). The speed of the adaptor stimuli was based on previous studies (e.g., Fornaciai et al., 2016) and was 20 deg/s in all except one condition, where speed was 5 deg/s. The reference and test stimuli had a speed of 10 deg/s (again in line with previous studies; e.g., Fornaciai et al., 2016). The temporal frequency of all the presented stimuli was broadband around 20 Hz or 5 Hz for the adaptor, and around 10 Hz for the reference and test stimuli, due to the broadband spectrum of spatial frequencies included in dot arrays. Motion coherence was 100% with leftward direction, except the condition where the adaptor direction was rightward. The stimuli were designed using the Psychophysics toolbox (Version 3; Kleiner et al., 2007) in Matlab (version r2015b; The Mathworks, Inc.).

2.3. Experimental design

The experiment included 6 blocks of 70 trials, all performed within a single experimental session. In each block, participants performed a duration discrimination task. With the exception of the baseline condition block, in all the rest of the blocks the duration discrimination was preceded by a perceptual adaptation phase (see below for more details). In the duration discrimination task, participants observed a reference and a test stimulus (always in this order), and had to report which one of the two lasted longer in time. The reference stimulus was always presented in the upper half of the screen centred on the vertical midline, with a vertical eccentricity of 5 deg from the centre of the screen, and its duration was always 500 ms. The test stimulus was always presented in the lower half of the screen with the same vertical eccentricity of the reference, and its duration was pseudo-randomly determined in each trial (300, 400, 500, 600 or 700 ms). To induce motion adaptation, an adaptor stimulus was presented before the reference stimulus according to different adaptation conditions based on the adaptor position, speed, and motion direction. In most of the conditions, motion adaptation was delivered in spatiotopic coordinates (i.e., adaptor and adapted stimulus matching in spatial, world-based coordinates), as this type of adaptation does not introduce spurious biases due to the distortion of perceived speed (e.g., Kanai et al., 2006; Fornaciai et al., 2016). Moreover, the properties of the different adaptor stimuli were chosen to result in effects of different strength, to have a parametric modulation of the adaptation-induced duration distortion. For instance, while adapt-

ing at high speed (20 deg/s) results in a strong effect, slower motion (5 deg/s) is expected to induce a weaker effect (e.g., Johnston et al., 2006). Similarly, while adaptation is most effective when adapted and adaptor stimuli move in the same direction, having the stimuli moving in opposite directions is expected to reduce the effect (Bruno et al., 2013). We thus chose the conditions we expected to result in graded effects: 20 deg/s motion adaptation with the adaptor in the same spatiotopic coordinates as the reference (20 deg/s spatiotopic adaptation; 20S), 20 deg/s spatiotopic adaptation with the adaptor moving in the opposite direction compared to the reference (20 deg/s inverse motion adaptation; 20I), and 5 deg/s spatiotopic adaptation (05S). In addition, as it has been widely used in previous studies yielding robust effects, we also tested 20 deg/s adaptation in retinotopic coordinates, i.e., with the reference matching the retinal position of the adaptor stimulus after an eye movement (20 deg/s retinotopic adaptation; 20R). Finally, we also included a condition in which the stimulus was presented in a neutral location not corresponding to either spatiotopic or retinotopic coordinates of the reference (20 deg/s notopic adaptation; 20N). This last condition is not expected to lead to duration distortions, and it was included to control for potential spurious effects of adaptation at the neural level. In addition to the adaptation conditions, we tested a baseline condition in which no adaptor was presented. To dissociate the different reference frames of adaptation, we asked participants to make a saccade during the interval between adaptor and reference, so that the subsequent reference position could correspond to the adaptor in terms of spatiotopic coordinates (fixed on the screen), in terms of retinal coordinates shifted by the eye movement, or none of the two (i.e., in the notopic condition). The stimulation sequence in each trial was therefore as follows: the trial started with the participant fixating on the first fixation point, located in the left half of the screen on the horizontal midline (horizontal eccentricity from the centre of the screen = 5 deg). The adaptor was presented in one of three different positions for 15 s in the first trial of the block, and then for 5 s in the rest of the trials (i.e., top-up adaptation). After 300-450 ms from the adaptation offset, the first fixation point disappeared and a second one appeared on the right side of the screen (horizontal eccentricity from the centre of the screen = 5 deg), cueing the participant to make a rightward saccade to the new fixation point (saccade amplitude = 10 deg). The reference stimulus was presented after 1 s from the onset of the second fixation point, to allow enough time to perform the saccade (i.e., the average saccade latency in untrained participants is expected to be, on average, around 200-250 ms; Fornaciai and Binda, 2015). Finally, the test stimulus was presented after 300–450 ms from the reference offset. At the end of the trial, the fixation point turned red, cueing the participant to provide a judgment, reporting which stimulus between the reference and the test lasted longer. Responses were provided by pressing the appropriate key (corresponding to “reference longer” or “test longer”) on a standard keyboard. After providing a response, the next trial started automatically after 1.3–1.45 s. The baseline condition involved a similar stimulus sequence, with the exception that no adaptor was presented before the reference. Each condition (i.e., different adaptation conditions and baseline) was performed separately in different blocks. The different blocks were separated by a break of at least 2 min to allow adaptation to decay. A block of trials took about 15 min, and the entire experimental session took about 90 min. See Fig. 1A for a depiction of the experimental procedure.

2.4. EEG recording and analysis

During each condition, EEG was recorded continuously using 32 active electrodes, evenly distributed over the entire scalp (with positioning and naming conventions following a subset of the extended 10–20 system) using a BioSemi ActiveTwo system (BioSemi, Amsterdam, The Netherlands) as well as an electro-oculogram (EOG) using the set-up described by Croft et al., 2005. The sampling rate was 2048 Hz.

The data preprocessing was performed using the functions of the EEGLAB toolbox for Matlab. First, the EEG signal was re-referenced offline from the original common mode sense reference (Van Rijn et al., 1991; CMS, positioned next to electrode Cz) to the average of two additional electrodes that were placed on the subject’s mastoids. Then, the continuous EEG signal was filtered using a 4th-order Butterworth band pass filter with range 0.5–45 Hz. To remove artifacts introduced by blinks and eye movements, EOG signals were recorded before the start of the session using four electrodes positioned around the right eye (Croft et al., 2005). Then, the EOG activity was used during the data preprocessing to remove eye artefacts following the Revised Artifact-Aligned Averaging (RAAA) procedure. The EEG data corresponding to the reference stimulus was epoched from -200 to 700 ms around its onset. The reference epochs were baseline-corrected using the 200-ms prestimulus interval and were examined to remove any remaining artefact. Baseline correction was applied to reduce the potential spurious effect of a lingering trace of the adaptor stimulus not related to the adaptation state itself. We also extracted the EEG signal corresponding to the top-up adaptor stimulus presentation i.e., 5 s of stimulus presentation and an additional 1-s interval after its offset. In the case of the top-up adaptor epochs, no baseline correction was applied to avoid a potential loss of information. To further remove artifacts, we also applied a rejection procedure based on an amplitude threshold, removing all trials in which the EEG amplitude exceeded $\pm$ 50 μV. Overall, 15% of the trials were excluded with this procedure.

The epoched EEG signal was analysed both in the time and the frequency domain. In the time domain, we focused on EEG activity time-locked to the reference stimulus, and computed ERPs by averaging all the reference epochs corresponding to each individual baseline and adaptation condition. In terms of ERPs, our primary target was the N200 component recorded at posterior EEG channels, which has been shown in previous studies to reflect motion processing and the effect of motion adaptation (Hoffmann et al., 1999; Hoffmann et al., 2001). In order to capture visual evoked responses to the reference and the N200 component, we thus selected a set of posterior occipito-parietal channels (O1, O2, PO4, PO3), and a main time window of interest consistent with the N200 (140–240 ms). Additionally, due to its potential involvement with time processing, we also assessed the CNV (contingent negative variation) component, using a time window from 250 to 500 ms, and selecting a set of fronto-central electrodes (FC1, FC2, Fz, Cz) that are typically associated with this component (Kononowicz and Penney, 2016; Li et al., 2017; Peters et al., 1977; Van Rijn et al., 2011).

In order to assess the effect of adaptation on EEG activity in the frequency domain and its relation to the distortion of perceived duration, we computed the difference in spectral power in the Beta frequency band during and after adaptation, compared to the unadapted condition (i.e., change in spectral power compared to the unadapted state). In this case, the preprocessing involved an additional band-pass filter with a range of 10–45 Hz. In this context, according to our initial hypotheses, we predicted that activity in the Beta band might be involved in mediating the distortion of perceived duration induced by motion adaptation. To address this hypothesis, we performed a series of spectro-temporal FFT analyses (100 ms sliding windows with 50 ms overlap) at different latency windows corresponding to the presentation of the adaptor and the reference stimulus. First, we focused on the top-up adaptation period performed in each trial (except the first) of each condition, and assessed the changes in power in the Beta (15–30 Hz) frequency band, compared to the unadapted condition. To do so we considered epochs time-locked to the onset of the 5-seconds period of adaptation (0-6 s, including 1 s after the adaptor offset). Moreover, Beta band power changes were assessed during the reference stimulus presentation. To further disentangle whether changes in Beta power occur during an early or late phase of the reference processing, or throughout its presentation, we assessed the Beta power separately in the first half (0–250 ms) and second half (250–500 ms) of the reference presentation. In both the case of the top-up and the reference epochs, the time-frequency analysis was

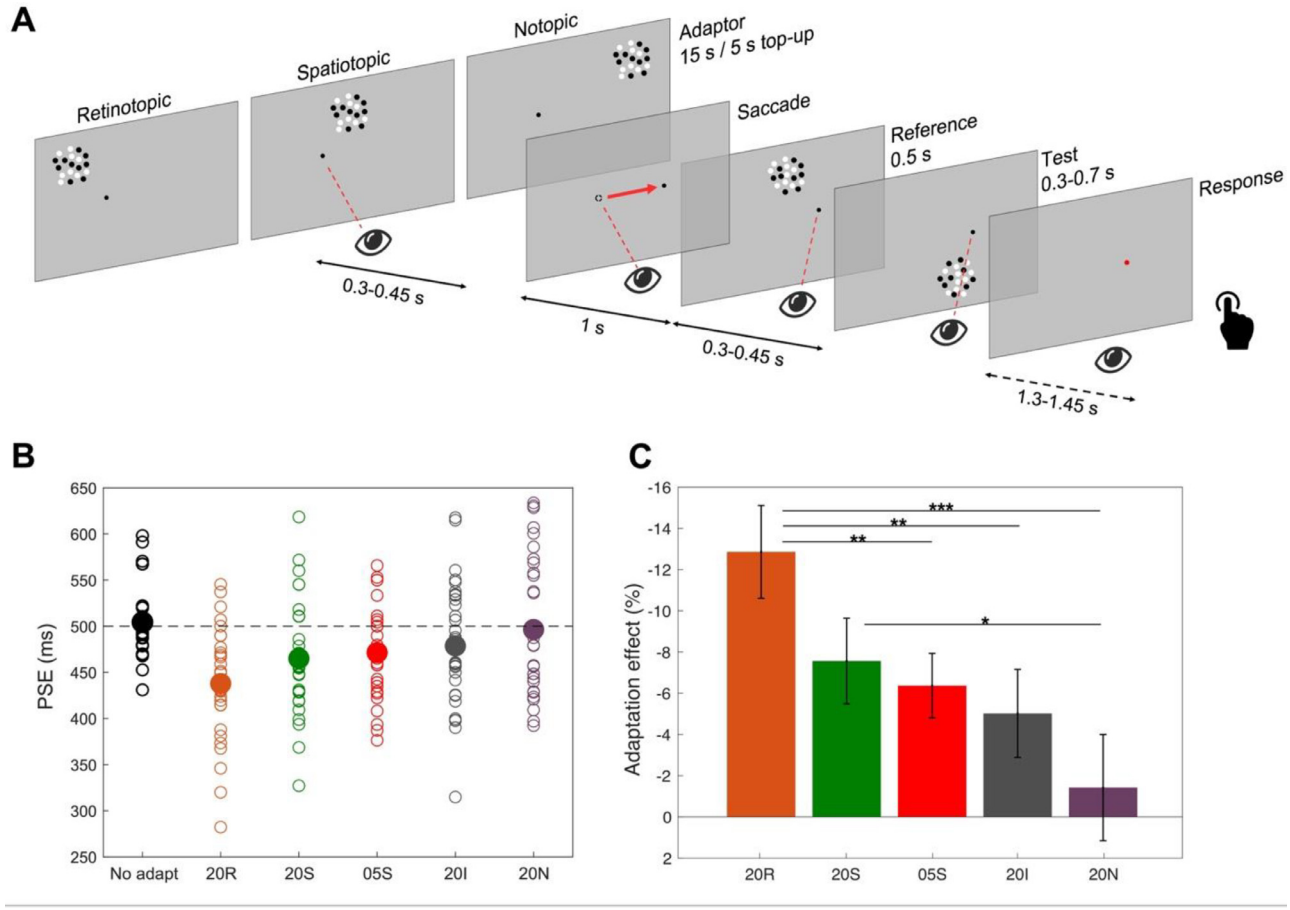

Fig. 1. Experimental procedure and behavioural results. (A) Schematic representation of the experimental paradigm, showing the three different positions of the adaptor according to the reference frame of the adaptation effect. The experimental procedure involved first an adaptation phase (15 s in the first trial, 5 s top-up in the following trials) in which a motion adaptor stimulus was presented on the screen. After the adaptation or top-up phase, the first fixation point (on the left part of the screen) was replaced by a second fixation point on the opposite side (right), 10 degrees away from the first one, cueing the participant to make a saccade on the new fixation. The reference stimulus was presented 1 s after the second fixation onset, and was followed by the presentation of the test stimulus. After the test, the fixation point turned red, and participants were instructed to indicate whether the reference or the test stimulus lasted longer. After providing a response, the next trial started automatically after 1.3–1.45 s. Note that the different adaptation conditions were tested in separate blocks of trials. (B) Individual (empty circles) and average (large filled circles) measures of PSE across the different conditions. (C) Behavioural effect of adaptation in terms of average adaptation effect index, across the different adaptation conditions. Effects are reported in terms of normalized difference of each condition against the unadapted condition, and represent the difference in the reference perceived duration caused by the different types of motion adaptation. Error bars are SEM. The codes on the x-axis correspond to the different adaptation conditions, i.e., 20R = 20 deg/s retinotopic adaptation, 20S = 20 deg/s spatiotopic adaptation, 05S = 5 deg/s spatiotopic adaptation, 20I = 20 deg/s inverse motion spatiotopic adaptation, and 20N = 20 deg/s notopic adaptation. Stars refer to the significance of paired t-tests. * $p < 0.05$, ** $p < 0.01$, *** $p < 0.001$.

performed on each trial separately, and power across the different frequency bands was computed as the average of all individual trials. The change in power was then computed as the difference in power in each adaptation condition compared to the power computed in the unadapted condition across a similar time window.

All the preprocessing, analytical procedures, and statistical tests were carried out in Matlab (The Mathworks, Inc.; version r2015b).

2.5. Behavioural data analysis

To assess the behavioural performance of each participant in the duration discrimination task, we fitted a logistic sigmoid function to the proportion of "test stimulus longer" responses as a function of the different test durations across all the trials of each condition. The fitting procedure was performed by means of the psignifit toolbox in Matlab, using the default fitting parameters. We then computed the point of subjective equality (PSE) as a measure of the perceived duration of the reference stimulus. This corresponds to the median of the sigmoid function and to the chance-level responses (i.e., 50% probability of responding that the test stimulus was longer). In order to estimate the change in perceived duration induced by adaptation, we computed an adaptation effect index as the difference in PSE between each adaptation condition and the baseline unadapted condition, normalized for the baseline and turned into percentage, according to the following formula:

$$\text{Adaptation effect} = \frac{1}{N}\sum_{i=1}^{N}\frac{\text{PSE}_i(\text{adaptation}) - \text{PSE}_i(\text{baseline})}{\text{PSE}_i(\text{baseline})} \times 100$$

Where N is the number of subjects. A negative adaptation effect means that the perceived duration of the reference stimulus (i.e., PSE) is shorter after adaptation compared to the baseline, thus indexing an underestimation, or "compression," effect. Conversely, a positive adaptation effect means that perceived duration increases after adaptation, compared to the baseline (i.e., overestimation). The significance of the adaptation effect in different conditions was tested with a one-sample t-test against a null hypothesis of zero effect. To assess whether there was a significant difference in the effect across different conditions we performed a one-way repeated measures ANOVA with factor "adaptation condition." Furthermore, a series of pairwise comparisons was per-

formed, comparing each condition against each other. In all cases, the α value of the tests was corrected for multiple comparisons.

2.6. EEG data analysis: modelling the relationship between temporal distortions and EEG signatures

The main goal of the present study was to address the relationship between the temporal distortions caused by adaptation, and the brain activity evoked by the adapted stimulus – in terms of both ERPs and spectral power – to understand the neural representation of perceived time. To address this relation, we used a series of linear mixed-effect (LME) models assessing whether either the modulation of ERPs or spectral power in the Beta frequency band predicts duration distortions. First, regarding the ERP analysis, we assessed the relation between the perceived duration of the reference stimulus (i.e., PSE), and the responses evoked by the adapted stimulus (i.e., the reference), according to the following model:

$$PSE \sim Condition + ERP * ROI + (1|subjects);$$

Where "PSE" represents the perceived duration of the adapted (reference) stimulus, "Condition" represents the adaptation condition, "ERP" represents the average amplitude of evoked responses within either the 140–240 ms latency window, corresponding to the N200 component, or the 250–500 ms window, corresponding to the expected CNV latency window (see *EEG recording and analysis*), and "ROI" represents the set of electrodes ipsilateral and contralateral to the stimulus position (only for the N200 analysis; see below). Indeed, our primary hypothesis when it comes to the relation between ERPs and the duration distortion concerned the motion-sensitive N200 component. In addition to that, however, we also assessed this relationship considering the CNV component, due to its potential, although debated, relationship with time perception (Kononowicz and Penney, 2016; Li et al., 2017; Peters et al., 1977; Van Rijn et al., 2011). Subjects were added to this model as the random effect. In the case of the analysis at the CNV latency window, however, we used an identical model with the exception of the ROI factor, since we used a single set of fronto-central electrodes (FC1, FC2, Fz, Cz).

Moreover, according to our second main hypothesis concerning the potential role of activity in the Beta frequency band, we assessed the relation between the magnitude of the adaptation effect, and the change in spectral power in the Beta frequency band, according to the following model:

$$Adaptation\ effect \sim Condition + Beta\ change * ROI + (1|subjects);$$

Where the "adaptation effect" is the normalised difference in PSE of each adaptation condition compared to the unadapted condition (see *Behavioural data analysis*), the "Beta change" factor represents the difference in spectral power in the Beta band, in each adaptation condition compared to the unadapted condition, and "ROI" represents the set of electrodes ipsilateral and contralateral to the stimulus position. This model was applied considering the change in spectral power computed at the offset of the top-up phase (considering a 1 s window after the offset). Finally, considering the change in Beta power during the presentation of the reference, we used the following model:

$$Adaptation\ effect \sim Condition + Beta\ change * ROI * Window + (1|subjects);$$

In this case, the fixed effect of time window ("Window") was added to assess the difference across the first (0–250 ms) and the second (250–500 ms) half of the reference stimulus presentation. In doing so, we aimed to assess the impact of adaptation on the processing of the reference stimulus at an early stage after its onset, and/or at a later stage towards its offset.

Note that in all cases the contralateral and ipsilateral electrodes represented by the ROI factor were selected based on the position of the stimulus relative to the fixation point, which, in the case of the adaptor stimulus, varied according to the reference frame of the adaptation condition (see Fig. 1A). For example, the channels PO3 and O1 were considered contralateral to the spatiotopic adaptor stimulus (which was presented on the right of the first fixation point), while the channels PO4 and O2 were selected as the contralateral channels to the retinotopic adaptor (presented on the left of the first fixation point).

The goodness of fit of the models used in the regression analysis was controlled by performing an ANOVA with type-III sums of squares (Satterthwaite's method) considering iteratively different models, including the full model and a series of nested models in which one of the factors is removed. In doing so, we thus assessed which version of the model minimises the residual sums of squares.

2.7. Data and experimental code availability

All the data generated in the experiment described in this manuscript and the experimental code are available on Open Science Framework at this link: https://osf.io/7kqvh/.

3. Results

The effect of motion adaptation on perceived time was tested with a behavioural paradigm in which we asked healthy human participants ($N = 32$) to discriminate the duration of pairs of visual stimuli after undergoing motion adaptation. The stimuli used in the duration discrimination task were arrays of moving dots, moving coherently from left to right at a speed of 10 deg/sec (for more details see *Materials and Methods*). The reference stimulus of fixed duration (500 ms) was presented in the upper visual quadrant, while the variable test duration (ranging from 300 to 700 ms) in the lower quadrant; both stimuli were centred on the vertical midline with a vertical (centre-to-centre) eccentricity of 5 degrees of visual angle from the middle of the screen. In the adaptation phase, prior to duration discrimination, participants were presented with a similar visual stimulus, from now on called the "adaptor," whose spatial position, speed, and motion direction relative to the reference stimulus was manipulated. Based on previous studies (Bruno et al., 2013; Burr et al., 2007; Fornaciai et al., 2016; Johnston et al., 2006) showing changes in perceived duration induced by motion adaptation depending on speed, motion direction and spatial position of the adaptor stimulus with respect to the reference, we decided to test the effect of motion adaptation in five different conditions. These conditions were: (1) 20 deg/s adaptation in which the adaptor and reference were in the same *retinotopic* coordinates (i.e., corresponding to the projected retinal position of the adaptor after an eye movement of 10 deg away from the first fixation point; 20R); (2) 20 deg/s adaptation in *spatiotopic* coordinates, in which adaptor and reference were in the same spatiotopic position (i.e., same position in screen coordinates; 20S); (3) 5 deg/s adaptation in spatiotopic coordinates (05S); (4) 20 deg/s spatiotopic adaptation, but with adaptor and reference moving in opposite directions (i.e., *inverse* motion condition; 20I); (5) 20 deg/s adaptation in a neutral location, that was neither the retinotopic nor the spatiotopic position of the reference stimulus (i.e., *notopic*; 20N). In most of the conditions, motion adaptation was delivered in spatiotopic coordinates (i.e., adaptor and adapted stimulus matching in spatial, world-based coordinates), as this type of adaptation does not introduce spurious biases due to the distortion of perceived speed (e.g., Kanai et al., 2006; Fornaciai et al., 2016). Moreover, the properties of the different adaptor stimuli were chosen to result in effects of different strength, to have a parametric modulation of the adaptation-induced duration distortion. Adaptation to a fast-moving stimulus presented in spatiotopic coordinates should lead to stronger adaptation effects compared to a stimulus moving at a lower speed (5 deg/s) or moving in an opposite direction compared to the adapted stimulus (Johnston et al., 2006; Bruno et al., 2013). Fast retinotopic adaptation was added to this set of conditions as it has proven to be very

effective in distorting perceived duration, although it is more prone to spurious effects related to perceived speed (Fornaciai et al., 2016). Finally, the notopic adaptation was used to further control for possible spurious effects at the neural level, as it is not expected to bias duration perception (i.e., due to the spatial selectivity of the effect). Note that not all the possible pairwise combinations of speed, reference frame, and motion direction were tested, but only the most important ones to get a sufficiently wide spectrum of effects. Besides the adaptation condition, duration discrimination performance was also measured in a baseline condition without adaptation (*unadapted* condition). A depiction of the experimental procedure is shown in Fig. 1A.

As a behavioural measure of the effect of motion adaptation on perceived duration, we focused on changes in the point of subjective equality (PSE; i.e., the duration of the test stimulus that is judged 50% of the times longer than the reference) across the different conditions. The average psychometric curves corresponding to the different conditions are shown in Fig. S1 (see the *Supplementary Materials*). To achieve a measure of the net effect of adaptation on duration estimates, we computed an adaptation effect index as the normalized difference in PSE between each adaptation condition and the unadapted baseline condition (see *Materials and Methods*). Fig. 1B shows the individual and average PSEs across the different conditions, while Fig. 1C shows the average adaptation effects. To assess the effect of adaptation on the reference perception we ran a one-way repeated measures ANOVA on the adaptation index. The analysis showed a significant effect of adaptation condition on participants' perception ($F(4,31) = 6.21$, $p < 0.001$, $\eta^{2} = 0.443$). To further explore this effect, we performed a series of one-sample t-tests against the null hypothesis of zero adaptation effect (Bonferroni-corrected α value equal to 0.01). The results showed a significant effect in the case of fast spatiotopic adaptation (20S; $t(31) = 3.64$, $p < 0.001$, Cohen's $d = 0.91$, average adaptation effect = 7.56%), retinotopic adaptation (20R; $t(31) = 5.7$, $p < 0.001$, $d = 1.43$, average effect = 12.86%), and in the slower spatiotopic adaptation (05S; $t(31) = 4.07$, $p < 0.001$, $d = 1.02$, average effect = 6.37%) condition. No significant effect was observed instead when adaptor and reference stimuli moved in opposite directions (20I condition; $t(31) = 2.35$, $p = 0.02$, $d = 0.58$, average effect = 5.02%), and when they occupied different spatial/retinal positions (20N condition; $t(31) = 0.5$, $p = 0.58$, $d = 0.14$, average effect = 1.42%). Moreover, we performed a series of paired t-tests comparing all the individual conditions against each other. In these tests, we considered a Bonferroni-corrected α equal to 0.0125 (i.e., considering the 4 tests needed to compare a given condition to all the others). The results (Fig. 1C) showed that the most robust duration compression effects were induced by fast (20 deg/s) adaptation in retinotopic and spatiotopic coordinates (20R and 20S condition). Namely, the effect in the 20R condition resulted to be significantly different from the 05S, 20I, and 20N condition ($p = 0.007$, 0.0012, and < 0.001, respectively), while the effect in the 20S condition was significantly different compared to the 20N ($p = 0.01$) condition. On the other hand, no other condition yielded effects significantly different from the control notopic (20N) condition (all $p > 0.0125$). No significant difference was observed between the 20S and 20R condition ($p = 0.02$). Overall, although these tests show that only the 20R and 20S adaptation conditions yielded effects significantly stronger than the 20N condition (which can be considered a control condition since no effect is expected), the effect sizes of the slow (5 deg/s; 05S condition) and inverse motion (20I condition) adaptation observed when running one-sample tests ($d = 1.02$ and 0.58, respectively) suggests that some genuine adaptation effect occurred also in those conditions. Individual measures of the adaptation effect across the group are shown in Fig. S2. The precision in the task (Weber fraction) across the different adaptation conditions is shown in Fig. S3 (see the *Supplementary Materials*).

At the neural level, our main goal was to assess the neural responses during the presentation of the reference stimulus – a physically identical stimulus that according to the preceding adaptation condition was perceived differently.

To assess the effect of adaptation at the neural level we looked at event-related potentials (ERP), and at changes in power in the Beta frequency band (15-30 Hz). Our main analyses primarily focused on the reference stimulus presentation. When assessing the effect in the frequency domain, we however deemed important to check for possible effects during adaptation and in the transition from adaptation to reference stimulus presentation.

First, according to our hypotheses, the adaptation-induced distortion of perceived duration might be associated to changes in brain activity related to motion processing. For instance, previous studies showed that the N200 component recorded at posterior EEG channels reflects motion processing, and it is sensitive to the effect of adaptation (Hoffmann et al., 1999; Hoffmann et al., 2001).

We thus started by analysing the event-related potentials (ERP) time-locked to the onset of the adapted reference stimulus, in a set of posterior occipito-parietal channels of interest (O2 and PO4 in the right hemisphere, O1 and PO3 in the left hemisphere). The average ERPs across channels contralateral to the reference stimulus (O2 and PO4), corresponding to the different adaptation conditions, are shown in Fig. 2A. As a first target latency window, we chose a window consistent with the timing of the N200 component (140-240 ms). Although the difference across different adaptation conditions is relatively small, the brainwaves plotted in Fig. 2A appear to be sorted according to the strength of the observed behavioural effects, and especially at around 200 ms after stimulus onset. Namely, the larger the duration underestimation, the smaller the deflection of the N200. The average ERP amplitude within the N200 latency window (140-240 ms) is shown in Fig. 2B. A one-way repeated measures ANOVA showed a main effect of adaptation condition on the N200 amplitude, suggesting that brain activity at the level of this component is modulated by the different adaptation conditions ($F(4,31) = 4.14$, $p = 0.001$, $\eta^{2} = 0.73$). We followed up the ANOVA with a series of paired t-tests comparing the N200 amplitude in each condition against each other (Bonferroni-corrected α value equal to 0.01). The results showed that the N200 amplitude in the baseline unadapted condition is significantly different (i.e., more negative) compared to all the other conditions ($t(31) = 4.09$-5.44, all $p < 0.001$) except the notopic condition ($t(31) = -2.72$, $p = 0.011$). Both the retinotopic and spatiotopic conditions showed a significant difference compared to the notopic condition ($t(31) = 4.45$, $p < 0.001$ and $t(31) = 3.12$, $p = 0.003$, respectively). No other comparison reached significance (max $t = 1.60$, min $p = 0.018$). The scalp topography of N200 displayed in Fig. 2C further shows that after all the adaptation conditions the response evoked by the reference tends to peak at electrodes contralateral to its position on the screen. The only exception to this pattern is the no-topic and the unadapted conditions, showing much less marked lateralization compared to the other conditions. This can be explained by the lack of duration compression in these adaptation conditions, suggesting again a relationship between the behavioural effect of adaptation and the activity in the N200 latency window. To better assess the relation between the N200 component and the behavioural effect of adaptation, we performed a linear mixed effect (LME) model analysis, using "Condition" (i.e., the different conditions performed by participants), the average N200 amplitude ("N200"), and "ROI" (i.e., channels contralateral vs. ipsilateral to the reference stimulus position; O2 and PO4, or O1 and PO3, respectively) as fixed effects, and participants as random effect (PSE ~ Condition + N200 * ROI +(1|subject)). The results from this regression model ($R^{2} = 0.47$, marginal $R^{2} = 0.24$) showed a significant effect of N200 ($\beta = 3.81$, $t = 2.34$, $p = 0.032$), a significant effect of condition ($\beta = 4.73$, $t = 2.96$, $p = 0.001$), and, importantly, a significant interaction between the N200 amplitude and the ROI ($\beta = 0.98$, $t = 1.28$, $p = 0.042$). The model used in the regression test was also compared to reduced (nested) models using an ANOVA, in which each of the factor is removed in an iterative fashion. We then assessed the residual sums of squares to evaluate which model explains more variance. The full model showed the lowest residual sums of squares compared to the reduced models, suggesting that the full model used in the actual analysis best fits

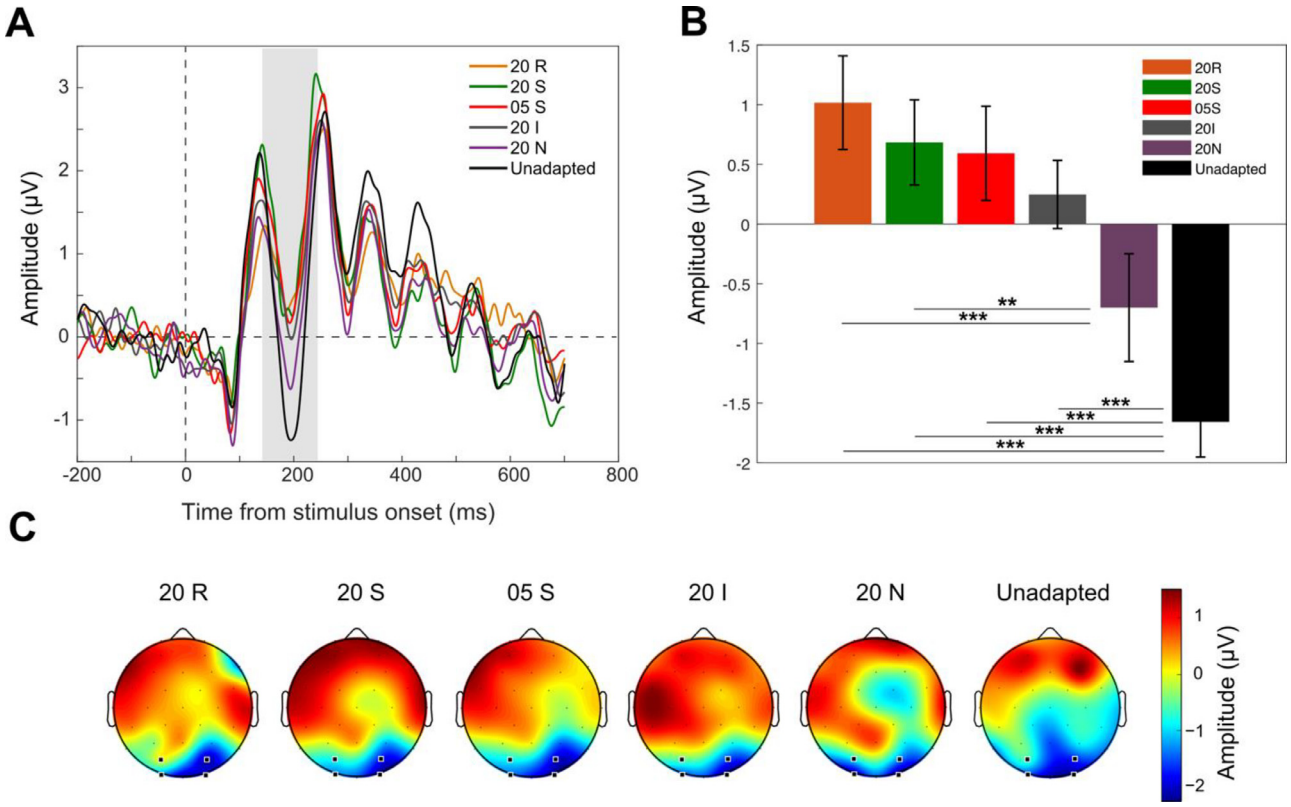

Fig. 2. ERPs at posterior channels and amplitude of the N200 component. (A) Event-related potentials (ERPs) recorded during the reference stimulus presentation, for each condition. The brainwaves shown here are computed as the average across all the target channels (O2, PO4, O1, PO3). The shaded area indicates the N200 time window (140–240 ms) used to compute the average amplitude. (B) Average ERP amplitude across the N200 time window, again considering the average of all the target electrodes (O2, PO4, O1, PO3). (C) Scalp distribution of activity averaged across the N200 time window (140–240 ms). Bold markers show the target channels considered in the analysis. Error bars are SEM. Stars refer to the significance of paired t-tests. ** $p < 0.01$, *** $p < 0.001$.

the data (see the Supplementary Table 1 for the full results). Moreover, we followed up this interaction by employing two simpler regression models (PSE ~ Condition + N200 + (1|subject)) within each ROI, which showed a significant effect of N200 at contralateral ($\beta = 4.14$, $t = 1.57$, $p = 0.01$) but not ipsilateral electrodes ($\beta = 0.15$, $t = 0.21$, $p = 0.83$). This supports the existence of a relationship between the N200 amplitude and the magnitude of adaptation-induced duration distortions, which is localised to the hemisphere contralateral to the stimulus.

Additionally, we also assessed another target latency window potentially associated with duration perception (Fig. 3). Namely, we assessed whether and to what extent behavioural performance could be predicted by activity in a later time window (250–500 ms after stimulus onset; Fig. 3A), corresponding to the expected latency of the contingent negative variation (CNV) component, usually observed at centro-frontal electrodes (FC1, FC2, Fz, Cz). Although debated, the CNV has been sometimes associated with temporal processing in previous studies (Kononowicz and Penney, 2016; Li et al., 2017; Peters et al., 1977; Van Rijn et al., 2011; Elbert et al., 1991; Pfeuty et al., 2003), and thus it may be involved also in this context. The analysis however showed no significant difference in CNV amplitude (Fig. 3) across the adaptation conditions (one-way repeated measures ANOVA: F (4,31) = 1.09, $p = 0.36$), and no predictive power of CNV amplitude on the behavioural performance (LME regression, $R^2 = 0.3$, average $\beta = 2.36$, $p = 0.48$). Fig. 3B shows the topographic distribution of average activity within the CNV window.

In addition to assessing the effect of adaptation in the time domain, we also tackled the signature of subjective time distortions from a different, complementary perspective. Namely, we further assessed the impact of adaptation in the frequency domain. In line with previous studies, our main hypothesis concerned the involvement of activity in the Beta frequency band in time perception. In this context we thus posited that the distortion of perceived time induced by adaptation might be related to changes in Beta frequency activity. Although our hypothesis mainly concerned the effect of adaptation on the reference stimulus and related changes in the Beta-band spectrum, we decided to look for possible changes in the frequency domain also during the top-up adaptor presentation. This decision was motivated by the possibility that the changes in brain activity leading to duration distortions may happen well before the onset of the reference stimulus, during the presentation of the adaptor stimulus itself.

First, we looked at the adaptation effect on the power of Beta-band activity in the 5 s top-up phase (the 5 s adaptation in each trial) and one second after its offset (Fig. 4A). Namely, we computed the power at frequencies around the Beta band (15–30 Hz) in a trial-by-trial fashion, and we computed a measure of change in power as the difference in the average power across trials compared to the unadapted condition. As shown in Fig. 4, we indeed observed a robust increase in power at frequencies corresponding to the Beta frequency band, throughout the top-up phase epoch. To assess this effect and its relation to the effect of adaptation measured behaviourally, we considered the average power in a latency window of 1 second after the offset of the top-up adaptor stimulus. First, a one-way repeated measures ANOVA showed a significant difference in the average change in Beta power (considering the 15-30 Hz range) after the offset of the top-up adaptor ($F(4,31) = 5.53$, $p < 0.001$, $\eta^{2} = 0.89$). We then performed an LME analysis considering the change in Beta power in such a 1-s time window after the offset of the top-up. The results of this regression model ($R^2 = 0.41$, marginal $R^2 = 0.23$) showed a significant effect of Beta change (β = -1.48, t = -

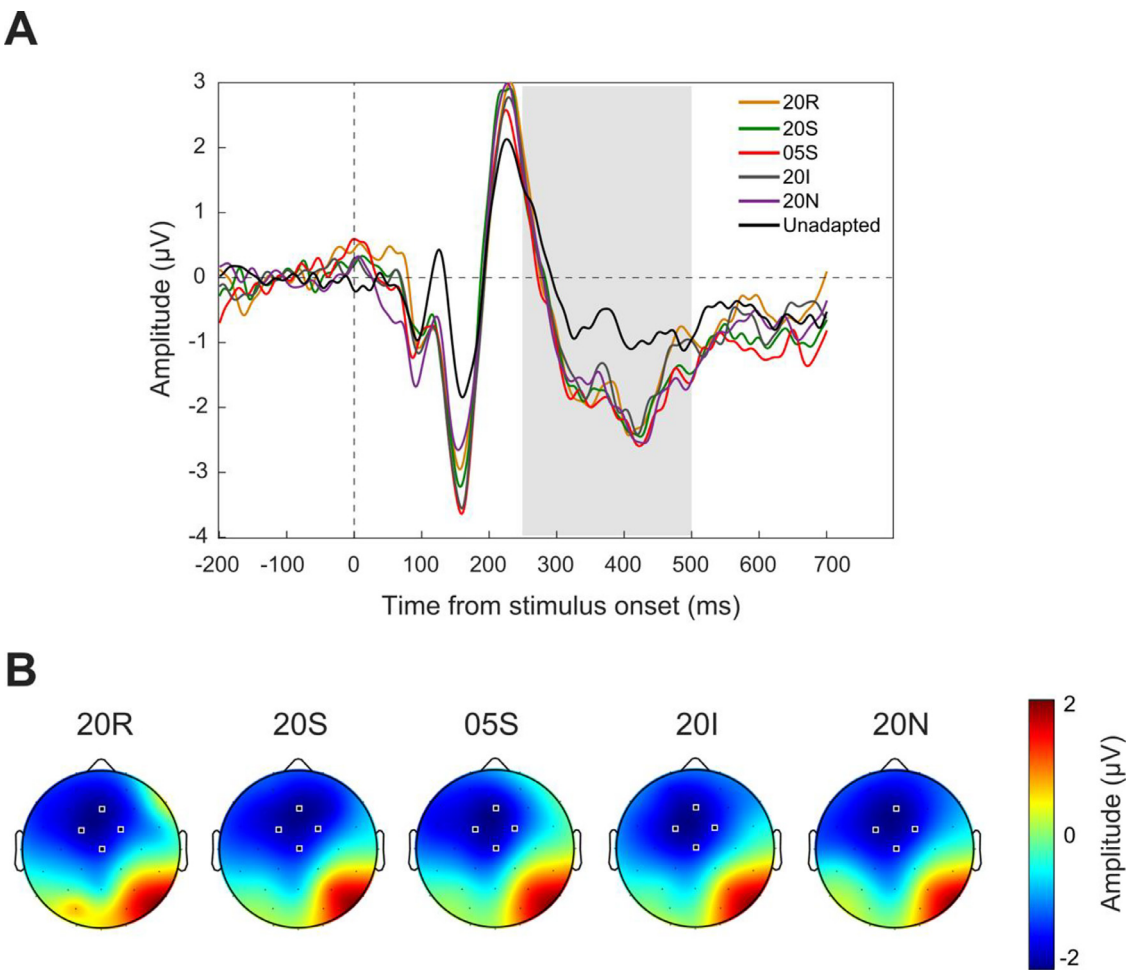

Fig. 3. CNV component. (A) Event-related potentials time-locked to the reference stimulus onset, corresponding to the different adaptation conditions, averaged across a set of fronto-central channels where the contingent negative variation (CNV) component is expected to peak (FC1, FC2, Fz, Cz). The shaded area indicates the time window of the CNV component used in our analysis (250–500 ms). (B) Scalp distribution of activity averaged across a time window corresponding to the typical timing of the CNV component. Bold markers show the target channels considered in the analysis.

2.06, $p = 0.031$), a significant effect of condition ($\beta = 4.96$, $t = 3.88$, $p = 0.001$), and a significant interaction between Beta change and ROI ($\beta = 1.76$, t = 2.05, $p = 0.031$). Also in this case, the goodness of fit of the model was assessed by comparing the residual sums of squares of the full model versus a series of reduced models in which one of the factors is removed iteratively. Again, the full model showed the lowest residuals sums of squares, suggesting that it fits the data better than the reduced models (see Supplementary Table 2 for the full results). To follow up the interaction observed in the regression results, we used again two simpler LME models within each ROI. In line with the previous analysis, the results showed a significant relation between the adaptation effect and the change in Beta power at contralateral ($\beta = -6.96$, $t = -3.35$, p = 0.001) but not ipsilateral ($\beta = 0.35$, $t = 1.02$, $p = 0.31$) electrodes.

Importantly, we also assessed whether the adaptation effect on spectral power was sustained during the subsequent presentation of the reference stimulus. Indeed, a genuine adaptation effect linked to the distortion in perceived duration observed behaviourally is expected to persist during the processing of the adapted stimulus (i.e., the reference). Again, we performed the time-frequency analysis in a trial-by-trial fashion, and then averaged the results before computing the change in power compared to the unadapted condition. As shown in Fig. 5A, the time course of spectral power changes around the presentation of the reference stimulus revealed a consistent increase in this frequency band. To further check whether the increase in Beta power changed over time and was more or less pronounced at early versus late latencies, we averaged the Beta power over two distinct time windows, one spanning from 0 to 250 ms (i.e., first half of the reference stimulus duration) and the other one from 250 to 500 ms after reference onset (i.e., second half of the reference stimulus duration). The rationale for assessing the effect on Beta power separately in the first and second half of the reference presentation was to further assess whether adaptation affects an early or a later phase of the reference stimulus processing, or both. As shown in Fig. 5B, we observed systematic changes in Beta power during the first half of the reference stimulus presentation, and these effects appeared to be greatest in the adaptation conditions leading to the strongest behavioural effects (i.e., 20 deg/s spatiotopic and retinopic condition, 20S and 20R). A one-way repeated measure ANOVA indeed showed a significant main effect of adaptation condition on changes in Beta power ($F(4,31) = 4.3$, p = 0.0236, $\eta^2 = 0.57$). A series of one-sample t-tests (Bonferroni-corrected $\alpha = 0.01$) further showed that the effect was significantly greater than zero in the 20S ($t(31) = 3.2$, $p = 0.0038$) and 20R adaptation conditions ($t(31) = 2.76$, $p = 0.0076$), while no significant effect was observed in the 20I, 20N, and 05S adaptation conditions ($t(31) = 1.89$, $p = 0.013$, $t(31) = 1.67$, $p = 0.02$ and $t(31) = 1.71$, $p = 0.015$ respectively). No significant difference was observed between the 20S and 20R condition (paired t-test, $t(31) = 0.285$, $p = 0.67$). In the second half of the reference presentation (250-500 ms), instead, no main effect of adaptation condition was observed (one-way repeated

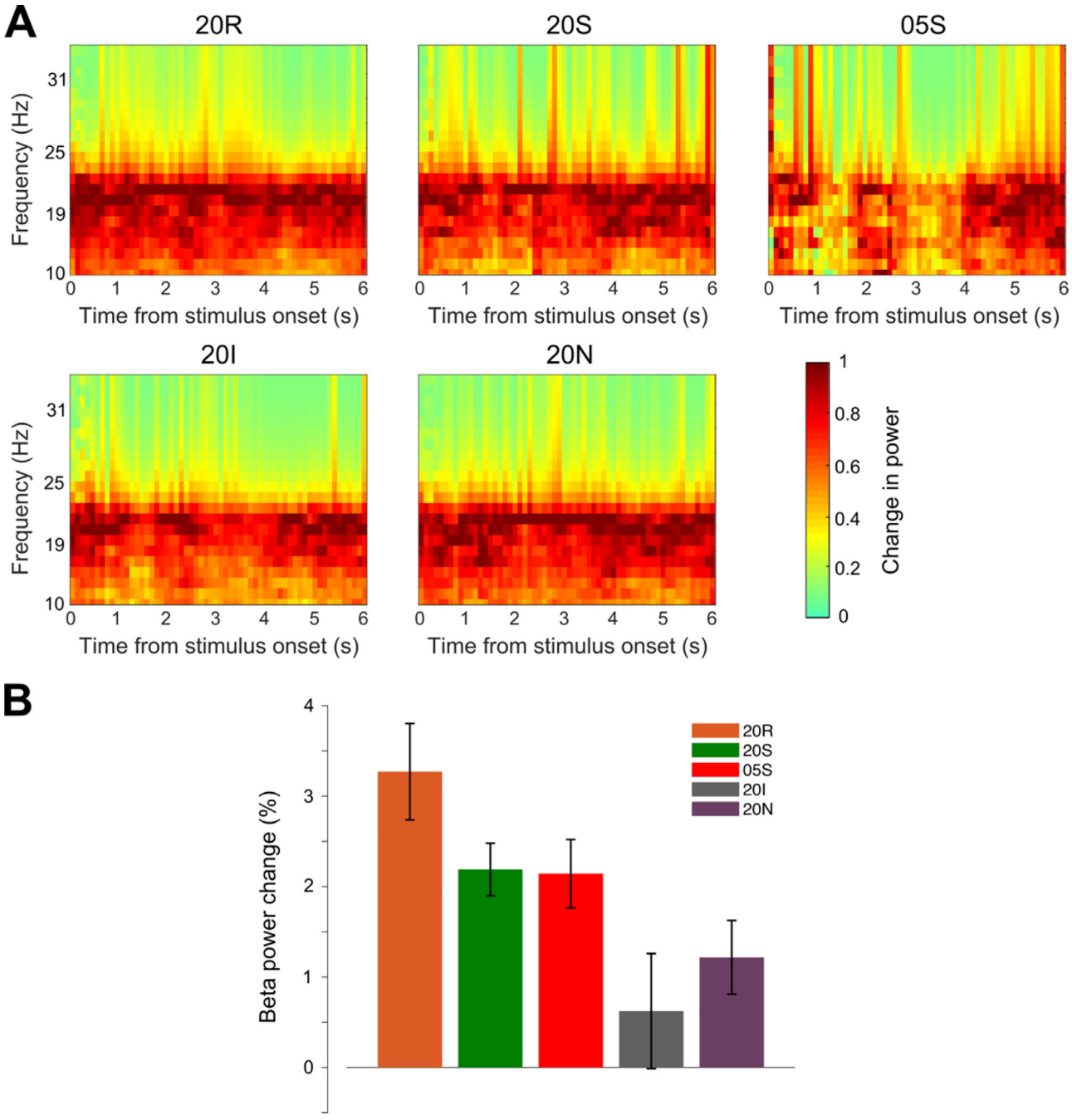

Fig. 4. Adaptation effect in the frequency domain during the top-up phase. (A) Changes in spectral power induced by adaptation compared to the unadapted state. The adaptation effect was assessed during the adaptation top-up phase and 1 sec after its offset, across all adaptation conditions. The spectral power was computed in a trial-by-trial fashion and then averaged, so that each plot shows the change in average power compared to the average of the unadapted condition. 0 marks the top-up onset (top-up duration is 5 s). (B) Average change in Beta power computed in the 1-second time window after the offset of the top-up adaptor stimulus. Error bars are SEM.

measure ANOVA, F (4,31) = 0.41, $p = 0.84$), and changes in Beta power were not significantly greater than zero in none of the adaptation conditions (one-sample t-tests, all $p > 0.05$).

We then assessed whether the perceptual effects induced by adaptation could be predicted by changes in Beta-band power during the first (0 to 250 ms after reference onset) and second (250 to 500 ms) half of the reference stimulus presentation. We performed a linear mixed effect regression analysis by fitting the following model: Adaptation effect ~ Condition + Beta change * ROI * Window + (1|subjects). The results ($R^2 = 0.47$, marginal $R^2 = 0.28$) showed a significant effect of Beta change (β = -27.66, t = -2.03, $p = 0.033$), a significant effect of condition (β = -6.62, t = -5.99, $p < 0.001$), and, more importantly, a significant three-way interaction between Beta change, ROI, and window (β = -23.41, t = -3.96, $p = 0.023$). Comparing the model used in the regression analysis with reduced models as in the previous cases, showed again that the lowest residual sums of squares is obtained with the full model. This suggests that the full model best fits the data, compared to the reduced models (see Supplementary Table 3). In this case, we followed up the interaction by using simpler LME models within each ROI and time window separately. In the first time window, we found again a significant relation between Beta change and adaptation at contralateral (β = -57.89, t = -3.38, $p < 0.001$) but not ipsilateral

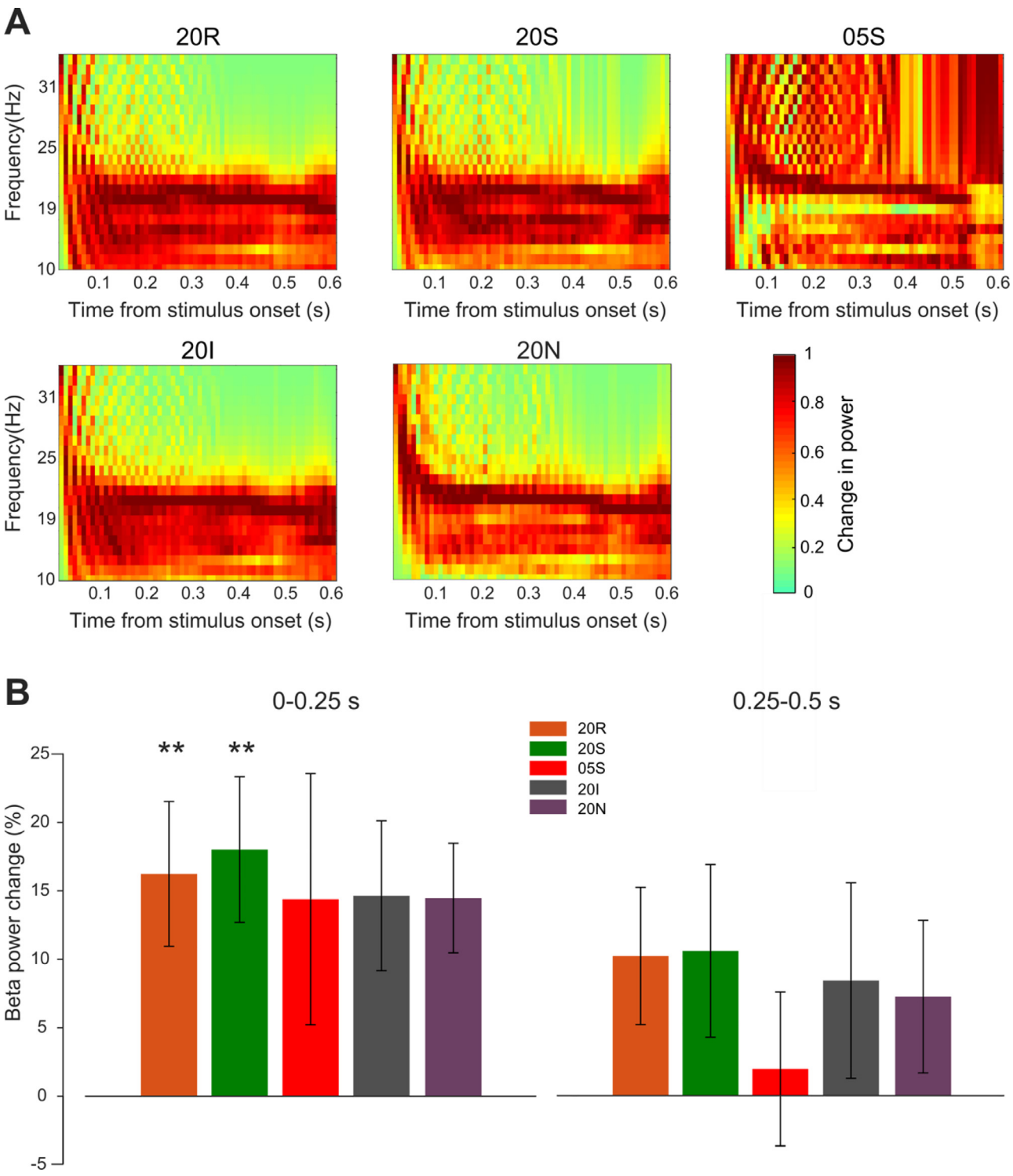

Fig. 5. Effect of adaptation on Beta-band activity during the reference stimulus presentation. (A) Changes in spectral power in all adaptation conditions compared to the unadapted state observed during the reference stimulus presentation across multiple frequency bands. (B)Average changes in Beta power during the reference stimulus presentation in its first half (left panel: 0–0.25 s after stimulus onset) and in its second half (right panel: 0.25–0.5 s). Error bars are SEM. Stars indicate the significance level of one-sample t-tests against zero, ** $p < 0.01$.

electrodes ($\beta = 1.04$, $t = 0.71$, $p = 0.48$). In the second time window, we did not find any significant relation, neither at contralateral electrodes ($\beta = 1.53$, $t = 0.66$, $p = 0.51$), nor at ipsilateral electrodes ($\beta = -1.2$, $t = -0.99$, $p = 0.32$). Similarly to the top-up adaptor offset, the change in Beta power measured during the first half of the reference presentation significantly predicted the perceptual bias measured behaviourally, with this effect emerging only from activity measured at contralateral channels. Conversely, no significant relation between adaptation effects and changes in Beta power was observed during the second half of the reference presentation, neither at contralateral nor at ipsilateral channels.

Finally, Fig. 6 shows the topographic distribution of Beta power changes at the time of top-up adaptation phase (Fig. 6A), and during the reference stimulus presentation (Fig. 6B). Looking at the scalp dis-

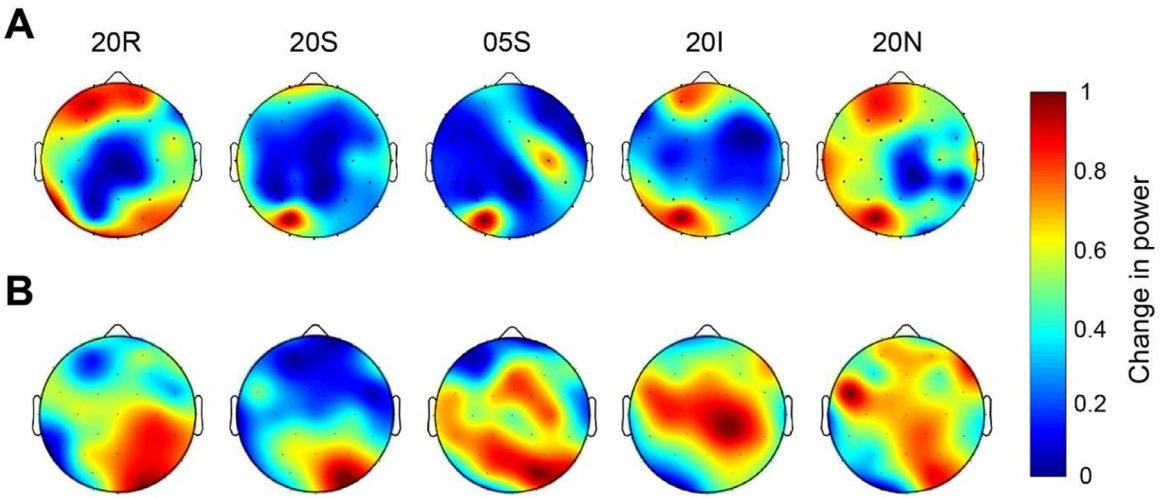

Fig. 6. Topographic plots of Beta power changes across the scalp. (A) Scalp distribution of Beta power changes during the top-up adaptation phase . (B) Scalp distribution of Beta power changes during the first half of the reference stimulus presentation.

tribution of Beta power increase during the presentation of the adaptor stimulus, there is a clear peak at occipito-parietal scalp locations contralateral to the stimulus position (i.e., left hemisphere for the spatiotopic and notopic condition, 20S, 05S, 20I, and 20N, right hemisphere for the retinotopic, 20R, condition). This suggests that the Beta power increase occurred in visual areas processing the adaptor stimulus. Interestingly though, the Beta power increase at the time of the reference presentation is instead evident, in most of the conditions (i.e., all except the 20R condition), in the opposite hemisphere compared to the effect during adaptation, at scalp locations contralateral to the reference stimulus position (see Fig. 6B). This last result suggests that the carry-over effect of adaptation is remapped to different neural populations after the gaze shift from the adaptor to the reference stimulus presentation.

4. Discussion

In this study, we investigated the neural correlates of perceptual time distortions induced by motion adaptation. Our results show that fast motion adaptation causes robust distortions in the perceived duration of the adapted reference stimulus, and these distortions are coupled with changes in brain activity measured with EEG. Specifically, we observed that modulations of the N200 component evoked by the reference stimulus and recorded in occipital electrodes contralateral to it, reflect the perceived duration of the adapted (reference) stimulus measured behaviourally. Moreover, we also observed robust and selective increases in Beta power during the adaptation (top-up) phase and during the first half of the reference stimulus presentation, which, crucially, could predict the perceptual duration compression effect. Overall, our results suggest that duration distortions induced by motion adaptation are associated with changes in brain activity that are (1) *local*, occurring in topographically-organized cortices processing the stimulus, and (2) *early*, as suggested by the N200 component and the Beta power modulation observed during the first half of the reference stimulus presentation.

Regarding the behavioural effect of adaptation, our results are consistent with earlier studies showing that fast motion adaptation causes a robust compression of the perceived duration of a subsequent stimulus (Ayhan et al., 2009; Bruno et al., 2010; Burr et al., 2007; Fornaciai et al., 2016; Johnston et al., 2006). Interestingly, we observed an effect in both retinotopic and spatiotopic coordinates. Although earlier studies observed effects in either one or the other of these reference frames (e.g., Burr et al., 2007; Johnston et al., 2006), effects emerging in both of them have been also reported (Fornaciai et al., 2016), suggesting that adaptation can occur at different levels of the processing hierarchy involving different reference frames. Moreover, besides the effect of 20 deg/s adaptation in retinotopic and spatiotopic coordinates, we also observed effects in the case of 5 deg/s and inverse motion adaptation, at least to some extent. However, the aim of the present study was not to understand which type of adaptation leads to duration distortion, but rather to modulate duration perception in a variety of conditions to assess the neural signature of such distortion.

Regarding the EEG results, we first show that the amplitude of the N200 ERP component is systematically modulated by adaptation at posterior scalp locations contralateral to the reference stimulus location (channel O2 and PO4). Importantly, such modulation predicts the distortion in perceived duration observed at the behavioural level. This finding suggests that the neural signature of adaptation is local, and likely occurs in topographically-organized visual areas. Interestingly, the N200 component has been previously linked to motion processing and adaptation (Hoffmann et al., 1999; Hoffmann et al., 2001), and it has been shown to arise from the motion area V5/MT (Probst et al., 1993). The modulation of the N200 component thus supports the idea of a crucial contribution to the adaptation effect of area V5/MT. On the other hand, no significant modulation has been observed at later latencies corresponding to the CNV component. Although sometimes associated with time perception (Macar and Vidal, 2009), the involvement of this component with the timing of external events is debated (e.g., Van Rijn et al., 2011). Our results may support the idea that the CNV is not a proper signature of interval timing or subjective duration. However, it is worth emphasizing here that our goal was to find differences linked to motion adaptation in ERP components time-locked to a stimulus of fixed duration (i.e., the 500-ms reference). For this reason, we cannot exclude the possibility that the lack of a clear CNV component is due to the fact that a constant stimulus may not be able to evoke a clear, measurable CNV.

Besides the ERP analysis, we also assessed the adaptation effect on spectral power in the Beta frequency band, compared to the non-adapted state. The results of this analysis show that the power of Beta activity gets substantially enhanced compared to the baseline unadapted condition, both after the offset of the top-up adaptation phase and during the first half of the reference presentation. Importantly, we show that such increase in Beta power predicts the magnitude of the behavioural adaptation effect on perceived duration, potentially in line with the idea of Beta-band activity playing a role in time perception (e.g., Kononowicz and Van Rijn, 2015; Kulashekhar et al., 2016).

What are the neural mechanisms underlying such increase in Beta power? The predictive power of brain activity in the Beta fre-

quency band in relation to perceptual distortions suggests an important role of Beta activity in temporal processing. Previous studies have indeed highlighted a role of the Beta band in temporal encoding (Kononowicz and Van Rijn, 2015; Kulashekhar et al., 2016). For instance, (Kononowicz and van Rijn, 2015) showed that Beta power can predict the duration produced by participants in a duration reproduction task. This was interpreted as reflecting motor inhibition processes modulating the reproduced duration. Our results further show that changes in Beta activity can be induced by visual adaptation, and these changes can predict the perceived duration of a visual stimulus in the absence of an explicit mapping of duration to a motor action. This supports the idea of an involvement of Beta activity in temporal processing independently from motor-related activity (see also (Kulashekhar et al., 2016), and further suggests a role of Beta activity in the representation of subjective time. Differently from Kulashekhar et al. (2016), where Beta changes were greater in fronto-central electrodes, the effect here emerged at occipital sites contralateral to the stimuli (i.e., either O1 and PO3 or O2 and PO4, depending on the position of the stimulus), again suggesting a close link between local changes in brain activity and duration perception.

Central to our findings is indeed that such modulation of Beta activity occurs in a local fashion. Interestingly, while the increase in Beta power occurs at channels contralateral to the adaptor, this effect shifts to the opposite hemisphere after a saccade. Indeed, at the time of the reference presentation, the peak increase in Beta power is evident at channels contralateral to the reference itself. Such a shift suggests that this effect is not a completely passive phenomenon – which should be strictly limited to the adapted neuronal population – but possibly involves an active process of remapping across different neuronal populations. This remapping may be linked for instance to the spatial coding of the adaptation effect, that may be spatiotopic rather than retinal (e.g., Cicchini et al., 2013). However, an exception to this pattern is the retinotopic condition, where we would have expected a shift in the opposite direction (i.e., from the right to the left hemisphere) to maintain the effect in a spatiotopic reference frame. The effect seems thus to occur in a local fashion, but without a stable coding in either retinotopic or spatiotopic coordinates – thus possibly reflecting a high-level process mediated by feedback signals from downstream areas, for instance.

Could these findings be trivially explained by differences in general visual processing instead of reflecting a distortion in subjective time? First, the fact that the reference stimulus was identical across all trials and conditions ensures that differences in brain activity could not be related to differences in the physical properties of the stimulus, but only to its perceived properties. However, motion adaptation may not uniquely affect perceived duration, but also other perceptual properties of the stimulus. For instance, perceived speed can be distorted by adaptation (e.g., Burr et al., 2007). However, adaptation effects concerning perceived speed or other low-level stimulus properties are expected to occur in a retinotopic reference frame only (Fornaciai et al., 2016). Since in most of our conditions adaptation was delivered in spatiotopic coordinates, it is thus less likely the EEG effects could be accounted for by other perceptual distortions.

It is important to note that while our data highlight a role of local and low-level visual processing in temporal distortions, it does not mean that the same pattern of effects would generalise to different contexts. The involvement of motion-sensitive ERPs, for instance, is likely related to the use of motion stimuli. In line with the idea of a widespread nature of neural timing mechanisms (Buonomano and Maass, 2009), we predict that using different stimuli would result in a different pattern of effects, involving local and low-level brain circuits specific to the task and the sensory modality of the stimuli at hand. An interesting question in this context is whether such early computations could in fact represent the stage at which our subjective sense of time actually emerges. Due to the complexity of perceived time and the many factors involved (e.g., as for instance the role of multisensory information; Heron et al., 2013), we believe that early perceptual processing is unlikely to be sufficient to fully explain time perception. However, a possibility is that this early stage might represent the starting point of a processing hierarchy culminating in our subjective perception of time.

Finally, although the adaptation paradigm employed here represents a powerful tool to induce a distortion in subjective duration and address its neural signature, it presents some limitations that should be acknowledged. One limitation concerns the eye movements performed after the adaptation phase, which were needed to test the spatial specificity of adaptation effects. These movements might have introduced a potential confounding factor due to the interaction between the motion profile of the adaptor (i.e., speed, direction, position) and the saccades themselves, since motion adaptation can affect the pattern of eye movements (Zimmermann et al., 2012). This, in turn, could have differently influenced the EEG responses in a condition-specific fashion. However, since eye artifacts have been removed during the EEG pre-processing and since the effect of motion adaptation should not depend on the specific properties of the saccades, we believe that this confounding factor could not fully explain the results obtained. Second, while our interpretation concerns the signature of subjective time, our paradigm did not allow to measure trial-by-trial perceived duration, but only an estimate based on the overall performance in each condition. A possibility is thus that our paradigm could capture aspects of time perception more related to decision than perceptual processing per se. Even if this remains a possibility, the spatial localisation of the adaptation effect (in electrodes contralateral to the reference stimulus) and its neural signature (for example the relatively early ERP activity related to motion processing) seem to support the idea that our results more likely reflect a change in perceptual processing rather than in decision-making.

To conclude, our results suggest that local and relatively low-level perceptual computations are involved in determining our subjective sense of time, supporting the contribution of early visual areas to the representation of perceived duration. Furthermore, we demonstrate the important role of Beta activity in predicting distortions of perceived time. Overall, these results thus support the idea that time perception is deeply rooted into the sensory/perceptual processing stream, and that Beta activity might reflect the routing of temporal information and the representation of subjective time.

Data and code availability statement

All the data generated in the experiment described in this manuscript and the experimental code are available on Open Science Framework at this link: https://osf.io/7kqvh/.

Declaration of Competing Interest

The Authors declare no conflict of interest related to the authorship of this manuscript.

Credit authorship contribution statement

Yelena Tonoyan: Conceptualization, Methodology, Formal analysis, Investigation, Data curation, Writing – original draft, Writing – review & editing, Visualization. **Michele Fornaciai:** Methodology, Formal analysis, Data curation, Writing – original draft, Writing – review & editing, Visualization, Funding acquisition. **Brent Parsons:** Conceptualization, Methodology, Software, Writing – review & editing. **Domenica Bueti:** Conceptualization, Methodology, Writing – original draft, Writing – review & editing, Supervision, Project administration, Funding acquisition.

Data availability

The data is freely available on an online repository. The link has been included in the manuscript.

Supplementary materials

Supplementary material associated with this article can be found, in the online version, at doi:10.1016/j.neuroimage.2022.119707.

References

Ayhan, I., Bruno, A., Nishida, S., Johnston, A., 2009. The spatial tuning of adaptation-based time compression. J. Vis. 9 (11), 1–12. doi:10.1167/9.11.2.

Brown, S.W., 1995. Time, change, and motion: the effects of stimulus movement on temporal perception. Percept. Psychophys. 57, 105–116.

Bruno, A., Ayhan, I., Johnston, A., 2010. Retinotopic adaptation-based visual duration compression. J. Vis. 10 (10), 30.

Bruno, A., Ng, E., Johnston, A., 2013. Motion-direction specificity for adaptation-induced duration compression depends on temporal frequency. J. Vis. 13 (12), 19. doi:10.1167/13.12.19.

Buonomano, D.V, Maass, W., 2009. State-dependent computations: spatiotemporal processing in cortical networks. Nat. Rev. Neurosci. 10 (2), 113–125.

Burr, D.C., Cicchini, G.M., Arrighi, R., Morrone, M.C., 2011. Spatiotopic selectivity of adaptation-based compression of event duration. J. Vis. 11 (2), 21. doi:10.1167/11.2.21, author reply 21a.

Burr, D., Tozzi, A., Morrone, M.C., 2007. Neural mechanisms for timing visual events are spatially selective in real-world coordinates. Nat. Neurosci. 10 (4), 423.

Cicchini, G.M., Binda, P., Burr, D.C., Morrone, M.C., 2013. Transient spatiotopic integration across saccadic eye movements mediates visual stability. J. Neurophysiol. 109 (4), 1117–1125.

Croft, R.J., Chandler, J.S., Barry, R.J., Cooper, N.R., Clarke, A.R., 2005. EOG correction: a comparison of four methods. Psychophysiology 42 (1), 16–24.

Elbert, T., Ulrich, R., Rockstroh, B., Lutzenberger, W., 1991. The processing of temporal intervals reflected by CNV-like brain potentials. Psychophysiology 28 (6), 648–655.

Fornaciai, M., Arrighi, R., Burr, D.C., 2016. Adaptation-induced compression of event time occurs only for translational motion. Sci. Rep. 6, 1–13. doi:10.1038/srep23341, August 2015.

Fornaciai, M., Binda, P., 2015. Effect of saccade automaticity on perisaccadic space compression. Front. Syst. Neurosci. 9. doi:10.3389/fnsys.2015.00127, September.

Fornaciai, M., Markouli, E., Di Luca, M., 2018. Modality-specific temporal constraints for state-dependent interval timing. Sci. Rep. 8 (1), 1–10.

Heron, J., Hotchkiss, J., Aaen-Stockdale, C., Roach, N.W., Whitaker, D., 2013. A neural hierarchy for illusions of time: duration adaptation precedes multisensory integration. J. Vis. 13 (14), 4. doi:10.1167/13.14.4, –4.

Hoffmann, M.B., Unsöld, A.S., Bach, M., 2001. Directional tuning of human motion adaptation as reflected by the motion VEP. Vis. Res. 41 (17), 2187–2194. doi:10.1016/S0042-6989(01)00112-2.

Hoffmann, M., Dorn, T.J., Bach, M., 1999. Time course of motion adaptation: motion-onset visual evoked potentials and subjective estimates. Vis. Res. 39 (3), 437–444. doi:10.1016/S0042-6989(98)00186-2.

Javadi, A.H., Aichelburg, C., 2012. When time and numerosity interfere: the longer the more, and the more the longer. PLoS One 7 (7), e41496. doi:10.1371/journal.pone.0041496.

Johnston, A., Arnold, D.H., Nishida, S., 2006a. Spatially localized distortions of event time. Curr. Biol. 16 (5), 472–479.

Johnston, A., Arnold, D.H., Nishida, S., 2006b. Spatially localized distortions of event time. Curr. Biol. 16 (5), 472–479. doi:10.1016/j.cub.2006.01.032.

Kanai, R., Paffen, C.L.E., Hogendoorn, H., Verstraten, F.A.J., 2006. Time dilation in dynamic visual display. J. Vis. 6 (12), 8.

Karmarkar, U.R., Buonomano, D.V., 2007. Timing in the absence of clocks: encoding time in neural network states. Neuron 53 (3), 427–438.

Kleiner, M., Brainard, D., & Pelli, D. (2007). *What's new in psychtoolbox-3?*

Kononowicz, T.W., Penney, T.B., 2016a. The contingent negative variation (CNV): timing isn't everything. Curr. Opin. Behav. Sci. 8, 231–237.

Kononowicz, T.W., van Rijn, H., 2015. Single trial beta oscillations index time estimation. Neuropsychologia 75, 381–389.

Kristjánsson, Á., Vuilleumier, P., Schwartz, S., Macaluso, E., Driver, J., 2007. Neural basis for priming of pop-out during visual search revealed with fMRI. Cereb. Cortex 17 (7), 1612–1624. doi:10.1093/cercor/bhl072.

Kulashekhar, S., Pekkola, J., Palva, J.M., Palva, S., 2016. The role of cortical beta oscillations in time estimation. Hum. Brain Mapp. 37 (9), 3262–3281.

Latimer, K., Curran, W., Benton, C.P., 2014. Direction-contingent duration compression is primarily retinotopic. Vis. Res. 105, 47–52.

Li, B., Chen, Y., Xiao, L., Liu, P., Huang, X., 2017a. Duration adaptation modulates EEG correlates of subsequent temporal encoding. Neuroimage 147 (2), 143–151. doi:10.1016/j.neuroimage.2016.12.015.

Macar, F., Vidal, F., 2009. Timing processes: An outline of behavioural and neural indices not systematically considered in timing models. Can. J. Exp. Psychol. Rev. Can. Psychol. Exp. 63 (3), 227–239. doi:10.1037/a0014457.

Meck, W.H., Benson, A.M., 2002. Dissecting the brain's internal clock: how frontal–striatal circuitry keeps time and shifts attention. Brain Cogn. 48 (1), 195–211.

Merchant, H., de Lafuente, V., Merchant, H., de Lafuente, V., 2014. Introduction to the neurobiology of interval timing. In: Neurobiology of Interval Timing. Springer, pp. 1–13.

Merchant, H., Yarrow, K., 2016. How the motor system both encodes and influences our sense of time. Curr. Opin. Behav. Sci. 8, 22–27. doi:10.1016/j.cobeha.2016.01.006.

Peters, J.F., Billinger, T.W., Knott, J.R., 1977a. Event related potentials of brain (CNV and P300) in a paired associate learning paradigm. Psychophysiology 14 (6), 579–585.

Pfeuty, M., Ragot, R., Pouthas, V., 2003. Processes involved in tempo perception: a CNV analysis. Psychophysiology 40 (1), 69–76.

Probst, T., Plendl, H., Paulus, W., Wist, E.R., Scherg, M., 1993. Identification of the visual motion area (area V5) in the human brain by dipole source analysis. Exp. Brain Res. 93 (2), 345–351.

Spencer, R.M.C., Karmarkar, U., Ivry, R.B., 2009. Evaluating dedicated and intrinsic models of temporal encoding by varying context. Philos. Trans. R. Soc. B Biol. Sci. 364 (1525), 1853–1863.

Togoli, I., Bueti, D., Fornaciai, M., 2022. The nature of magnitude integration: contextual interference vs. active magnitude binding. J. Vis..

Togoli, I., Fornaciai, M., Bueti, D., 2021. The specious interaction of time and numerosity perception. Proc. R. Soc. B Biol. Sci. 288 (1959), 20211577. doi:10.1098/rspb.2021.1577.

Treisman, M., Faulkner, A., Naish, P.L.N., Brogan, D., 1990. The internal clock: evidence for a temporal oscillator underlying time perception with some estimates of its characteristic frequency. Perception 19 (6), 705–742.

Van Rijn, A.C.M., Peper, A., Grimbergen, C.A., 1991. High-quality recording of bioelectric events. Med. Biol. Eng. Comput. 29 (4), 433–440.

Van Rijn, H., Kononowicz, T.W., Meck, W.H., Ng, K.K., Penney, T.B., 2011a. Contingent negative variation and its relation to time estimation: a theoretical evaluation. Front. Integr. Neurosci. 5, 91.

Wiener, M., Matell, M.S., Coslett, H.B., 2011. Multiple Mechanisms for Temporal Processing. Front. Integr. Neurosci. 5. doi:10.3389/fnint.2011.00031.

Xuan, B., Zhang, D., He, S., Chen, X., 2007. Larger stimuli are judged to last longer. J. Vis. 7 (10), 2.

Zimmermann, E., Morrone, M.C., Burr, D., 2012. Visual motion distorts visual and motor space. J. Vis. 12 (2), 10. doi:10.1167/12.2.10, –10.